Hyperfine Interactions 76 (1993) 221–232

Pure multipoles from strong permanent magnets: analytic and experimental results

W.G. Kaenders, V. Frerichs, F. Schröder and D. Meschede

Institut für Quantenoptik, Universität Hannover, 3000 Hannover 1, Germany

We present the construction of arbitrary multipole field configurations from strong permanent magnets for trapping charged or neutral particles. A general analytic method for the design of three-dimensional magnetic multipoles is discussed for an idealized continuously varying magnetisation taking advantage of the superposition principle. Simple recipes for constructing magnetic dipole and quadrupole fields are given with two types of elements, axially and radially magnetised rings. Cylindrical magnet components not only give free access to the experimental region of interest, but also allow for some tunability to reduce undesirable higher multipole orders. Measurements confirm theoretical predictions achieving useful magnetic fields of 1 T and steep gradients of 3 T/cm with high purity over several ccm.

1. Introduction

Magnetic fields of appreciable strengths and good homogeneity are requested in a variety of spectroscopic applications as for example ion trapping or nuclear magnetic resonance spectroscopy. For stable trapping of light particles of mass m and charge e in a Penning ion trap with a homogeneous magnetic field B one has to fulfill the condition that the cyclotron frequency $\omega_c = eB/m$ supersedes the axial frequency $\omega_z = \sqrt{2eV/mr_0^2}$ by at least a factor of $\sqrt{2}$ [1]. For the trapping of e^-, p, e^+, $\bar{p}$, and even the lighter elements (H^-, $Li^{\pm}$, ...) a permanent magnet assembly can provide sufficient field strength of order 1 T to operate a Penning trap well in the stable regime.

Another potential application of permanent magnets is the trapping of neutral particles in quadrupole or hexapole traps. Spherically symmetric arrangements with the inevitable B field zero in the middle as well as Ioffe-type traps [2–4] or complete rings are feasible and have been discussed by several authors [5,6]. Up till now all these traps have been built with superconducting coils. Operation and maintenance is very expensive and laborious. With the application of permanent magnets the field may be opened to research groups living on more restricted budgets.

While the potential depth of static magnetic traps will not much exceed the equivalent of $E_{max} = \mu_B B/k \leqslant 1$ K, laser manipulation of neutral elements (in parti-

cular alkaline and earth alkaline metals, metastable rare gas atoms) has advanced tremendously. Hence one can hope to load precooled atoms into a magnetic structure, though this does neither include hydrogen nor antihydrogen currently. By time coordinated optical pumping from the high field seeking state into the trapped "low field seeker" state one should obtain good loading rates either from a laser cooled atomic beam or a magneto-optical trap (MOT) [7].

In this contribution to the Antihydrogen Workshop we want to report on cylindrically symmetric, iron-free magnetic configurations. Halbach has pioneered the understanding and application of permanent magnets for experiments, mainly in accelerator physics (e.g. ref. [8]). We briefly discuss important properties of rare earth magnets (REM). Subsequently, we will be focussing on the construction of magnetic dipoles and quadrupoles from permanent magnets. Owing to the appealing properties of modern permanent magnetic material, a fully analytic treatment is possible. We present cylindrical ring configurations allowing good access to the inner field region and hence of predominant experimental interest.

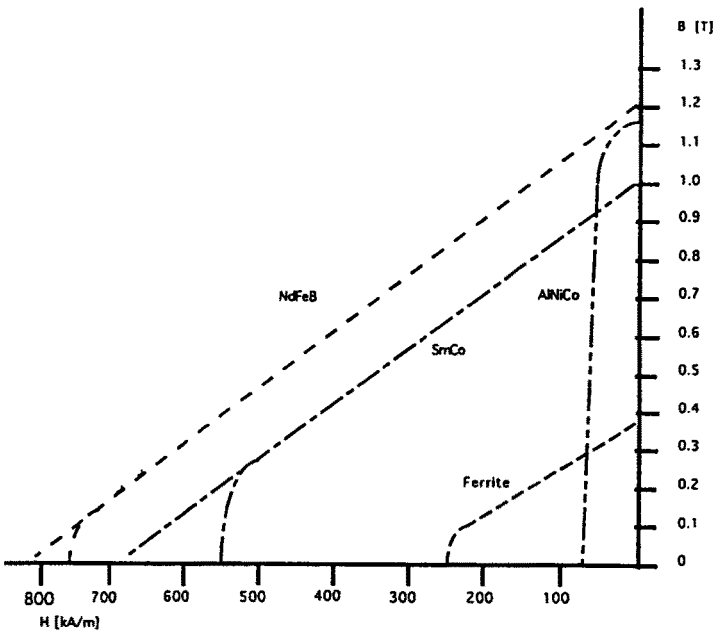

Fig. 1. Schematic $B(H)$ diagrams in the II. quadrant: rare earth materials (REM) have both high remanence $B_r = B(H = 0)$ and high coercitive force $H_c = H(B = 0)$. The magnetic permeability μ_r is linear and of order $\mu_0^{-1}\partial B/\partial H = \mu_r \approx 1$.

2. Discussion of REM properties

The magnetic material can be characterized by the second quadrant of the $B(H)$ curve (fig. 1). The wellknown connection between the magnetic induction $\boldsymbol{B}$, the magnetic field $\boldsymbol{H}$ and the magnetisation $\boldsymbol{M}$ is given (in SI units) as $\boldsymbol{B} = \mu_0(\boldsymbol{H}+\boldsymbol{M}) = \mu_r\mu_0\boldsymbol{H}$, where μ_0 and μ_r are the vacuum and the relative permeability.

To understand material properties of rare earth magnets (REM), in the first place SmCo (remanence $B_r \approx 1.0$ T) or NdFeB ($B_r \approx 1.2$ T), some fundamental knowledge of the manufacturing process is helpful. Starting from a powder of the wanted chemical composition the material is first pressed and then sintered within a weak homogeneous field. Through orientation of the crystallites a strong macroscopic anisotropy is introduced into the material. The resulting raw block (typically $50 \times 50 \times 100$ mm^3) is very brittle, only weakly magnetic and can be machined by grinding, drilling and, most conveniently, by wire-erosion. The magnet can be charged to full strength in a final step by a strong, pulsed magnetic field (typically 4000 kA/m) exclusively in the anisotropy direction.

Although it is in principle possible to manufacture a specific magnetic structure with varying magnetisation by processing the raw material in an appropriate external field, the effort is prohibitive. Therefore suitably formed blocks of uniform magnetisation are assembled in order to approximate a continuously varying direction of magnetisation.

The anisotropy of the material and, after charging the magnets, the magnetisation can never be truly uniform for a full block. The block's own magnetic field causes distortions at the outer parts of the block, and small distortions of the direction of the magnetisation up to some degrees are inevitable. However, besides preselection the field errors can be kept small by locating the various "oblique" parts within the assembly so that their contributions cancel [9]. This of course requires good knowledge of the magnetic properties of each individual segment, such as direction and magnitude of the total magnetic dipole moment.

Outgassing rates were shown to be smaller than 10^{-8} mbar ℓ/cm s for SmCo and even better for NdFeB [10] which allows their use within an ultrahigh vacuum. Unfortunately the materials cannot be heated to more than about 80°C (NdFeB) or 100°C (SmCo) without being affected by drastic irreversible demagnetisation. While baking out the UHV vessel the magnet assembly has to be cooled. For future experiments at a pressure of 10^{-10} mbar we plan to cool the magnets down below liquid nitrogen temperature during the course of the experiment. The surface now will work to our benefit supplying good cryopumping ability. The remanence and coercitivity fields of the REM will even be increased.

In the range between 20 and 80°C the reversible temperature coefficient of the magnetisation is of the order 10^{-3}/K. The reversible permeability μ_r at room temperature is very close to 1, $\mu_r \approx 1.1$ [11].

3. Analytic treatment

The intuitive concept underlying our analytic treatment is: How do we have to position and orient a piece of magnetic material in a given coordinate system so that it contributes maximally to a given multipole at the origin?

Magnetostatics can be treated very much the same way as electrostatics: $\nabla \times \boldsymbol{H} = 0$ and $\nabla \cdot \boldsymbol{B} = \mu_0 \nabla \cdot \boldsymbol{H} = 0$ and hence outside the material we can find a scalar potential Φ which obeys Laplace's equation, $\Delta\Phi = \nabla \cdot \boldsymbol{M}$, where $\boldsymbol{M}(\boldsymbol{r})$ is the magnetisation of the material. If $\boldsymbol{M}$ is known, as it is the case for REMs, the potential may be calculated from [12]

$$\Phi = -\frac{\mu_0}{4\pi} \int_V \frac{\boldsymbol{M}(\boldsymbol{r}') * (\boldsymbol{r} - \boldsymbol{r}')}{|\boldsymbol{r} - \boldsymbol{r}'|^3} \mathrm{d}^3 r . \tag{1}$$

In spherical coordinates $r\theta\phi$ the potential of a pure axial field multipole or order $2n$ can be written as

$$\Phi_n(r) = \Phi_0 r^n P_n(\cos\theta) . \tag{2}$$

As usual we expand Φ in a multipole series with convergence radius $r < r'$,

$$\Phi = B_r \sum_l^{\infty} C_l r^l P_l(\cos\theta) . \tag{3}$$

A pure multipole of order $2l$ has $C_{2l} = 0$ for $l \neq 2n$.

For our calculations we assume that $\mu_r = 1$, and furthermore coercitive forces large enough to prevent demagnetisation. In this case the magnetisation is independent of the magnetic field, an approximation which is well justified for REM materials and a precondition for the application of the superposition principle. For azimuthal magnetisations of constant magnitude $|\boldsymbol{M}| = M_0 = B_r/\mu_0$,

$$\boldsymbol{M} = M_0 \cos(\alpha - \theta')\boldsymbol{e}_r + M_0 \sin(\alpha - \theta')\boldsymbol{e}'_\theta , \tag{4}$$

the solution can be given in integral form, where α is the angle between the z-axis and the magnetisation axis (fig. 2).

The full calculation is explicited in ref. [13]. Here we summarise the results only and discuss them with respect to their applications in trapping of charged or neutral particles.

The coefficients C_l^{α} of eq. (3) for magnetisations $\boldsymbol{M}$ of the form in eq. (4) can be calculated most efficiently in spherical coordinates even though the magnet geometry is cylindric,

$$C_l^{\alpha} = \tfrac{1}{2} \int_{\rho_1}^{\rho_2} \rho' \,\mathrm{d}\rho' \int_{z_1}^{z_2} \mathrm{d}z' \frac{1}{r'^{l+2}} \{ -(l+1)\cos[\alpha(\rho', z')] P_{l+1}(\cos\theta') + \sin[\alpha(\rho', z')] P_{l+1}^1(\cos\theta') \} . \tag{5}$$

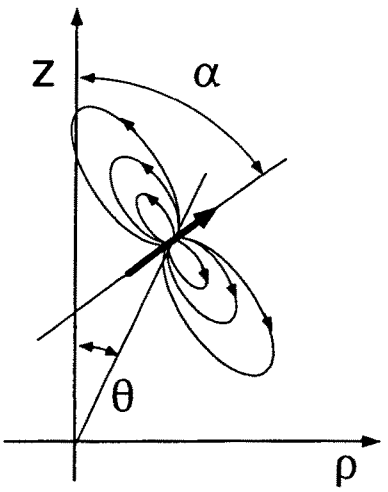

Fig. 2. Direction of magnetisation for a volume element in spherical coordinates. The magnetisation has no ϕ-component.

In eq. (5) C_l is a function of the angle α, $C_l = C_l^{\alpha}$. Maximum contribution to a multipole of order $2l$ is achieved for an angle α which obeys

$$\tan\alpha(\theta') = -\frac{1}{l+1}\frac{P_{l+1}^{1}(\cos\theta')}{P_{l+1}(\cos\theta')}. \tag{6}$$

Since it is technically impossible to continuously vary the angle α, we exploit the general formulae for two special cases only: axially and radially magnetised cylinders. Every given azimuthal magnetisation without tangential contributions can be decomposed into a superposition of these two cases. For axially magnetised rings ($\alpha = 0, \pi$) only the cos-terms survive and the sine-terms are left over for the radially magnetised cylinder ($\alpha = \pm\pi/2$). Explicit formulae can be given for both cases [13]. We give here the first three coefficients for semiinfinite cylinders ($z_1 = z, z_2 = \infty$), which will be referred to in the following discussion,

$$C_1^0 = \frac{1}{2}\frac{z}{(\rho^2+z^2)^{1/2}}\bigg|_{\rho_1}^{\rho_2}, \quad C_1^{\pi/2} = \frac{1}{2}\left(\frac{\rho}{(\rho^2+z^2)^{1/2}} - \ln[\rho + (\rho^2+z^2)^{1/2}]\right)\bigg|_{\rho_1}^{\rho_2}, \tag{7}$$

$$C_2^0 = -\frac{1}{4}\frac{\rho^2}{(\rho^2+z^2)^{3/2}}\bigg|_{\rho_1}^{\rho_2}, \quad C_2^{\pi/2} = -\frac{1}{4}\frac{\rho^3}{z(\rho^2+z^2)^{3/2}}\bigg|_{\rho_1}^{\rho_2}, \tag{8}$$

$$C_3^0 = -\frac{1}{4}\frac{z\rho^2}{(\rho^2+z^2)^{5/2}}\bigg|_{\rho_1}^{\rho_2}, \quad C_3^{\pi/2} = -\frac{1}{12}\frac{\rho^3(\rho^2+4z^2)}{z^2(\rho^2+z^2)^{5/2}}\bigg|_{\rho_1}^{\rho_2}. \tag{9}$$

The superposition principle gives immediate access to cylinders of finite length. Note that the coefficients of course reflect the symmetry of the underlying problem.

Using recurrence relations for the Legendre polynomials we obtain a useful connection between the C_l-coefficients of adjacent order and identical orientation α

$$C_{l+1}^{\alpha} = -\frac{1}{l+1}\frac{\partial}{\partial z}C_l^{\alpha} \tag{10}$$

and between the axial ($\alpha = 0, \pi$) and radial ($\alpha = \pm\pi/2$) case

$$C_l^{\pi/2} = (l+1)\int_{\rho_1}^{\rho_2} \mathrm{d}\rho\, \chi_{l+1}^{0}\,, \tag{11}$$

where χ_l is the indefinite integral in ρ corresponding to the definite integrals given in eqs. (7)–(9). In figs. 3 and 4 we give two examples of stacked cylindrical ring assemblies for dipole and quadrupole field configurations, respectively.

4. Optimisation strategies

In order to maximise the dipole field strength we have to maximise the C_1-coefficient. Adding to the stack a thin layer Δz of a magnetic ring with magnetisation angle α ($\alpha = 0, \pm\pi/2, \pi$) results in a change ΔC_1^{α}. From eq. (9) we know that the C_2^{α}-coefficient as a function of z is proportional to the change $\Delta C_1^{\alpha} = 2C_2^{\alpha}\Delta z$. Always choosing the angular orientation α with maximum C_2^{α} and integrating from the symmetry point 0 to a length z we find the optimum composition of such a dipole stack (fig. 3).

In principle the dipole can be made infinitesimally strong ($B \propto B_r \ln(\rho_i/\rho_a)$) but the approximations we made for the magnetic material will break down as soon we come close to the coercitive field strength leading to irreversible demagnetisation. In our example we have inserted realistic diameters and have shown that magnetic fields of the order of the remanence B_r of the material can be achieved easily.

For a strong magnetic quadrupole field we follow the former argument, and study the C_3^{α}-coefficients as a function of z in order to maximise the quadrupole field strength at the origin. Here the principal limit is [13]

$$\left(\frac{\mathrm{d}B}{\mathrm{d}z}\right)_{\max} = 2.4B_r/\rho_i\,. \tag{12}$$

Fig. 4 shows a construction and corresponding evaluation for realistic inner and outer diameters.

5. Experiments

The theoretical predictions were tested with a set of axially and radially magnetised rings of the inner and outer diameters given in the figures.

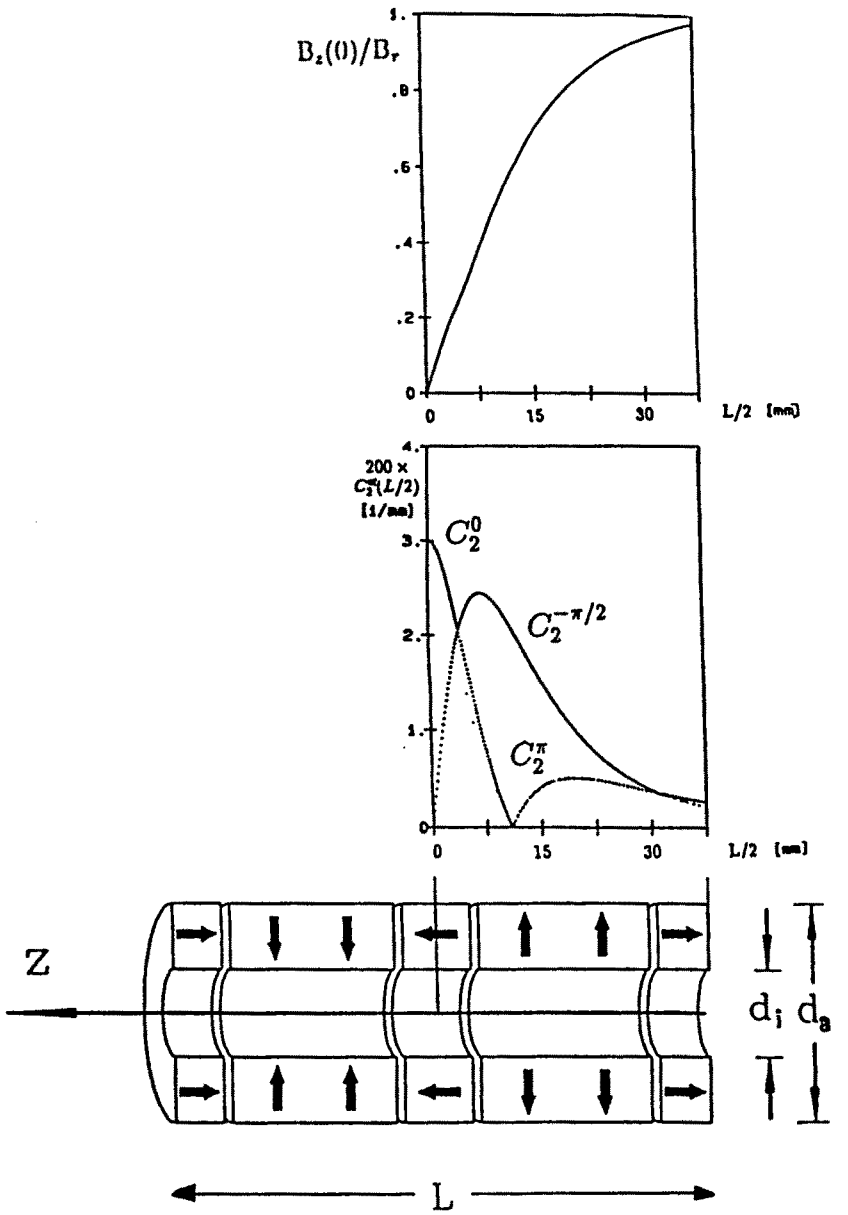

Fig. 3. Stacked cylindrical magnets ($d_i = 20$ mm, $d_a = 50$ mm) for maximum dipole field strength at the origin located at the middle of the assembly: an axially magnetised ring ($\propto C_2^0$) contributes maximally in the $z = 0$ plane but with increasing length of the stack radially magnetised rings ($\propto C_2^{\pi}/2$) become more favourable. For $L/2 \geqslant 30$ mm a ring with magnetisation opposing ($\propto C_2^{\pi}$) the first one at the origin should be used. The curve on top shows the overall achievable field strength in units of the field remanence B_r as a function of total length.

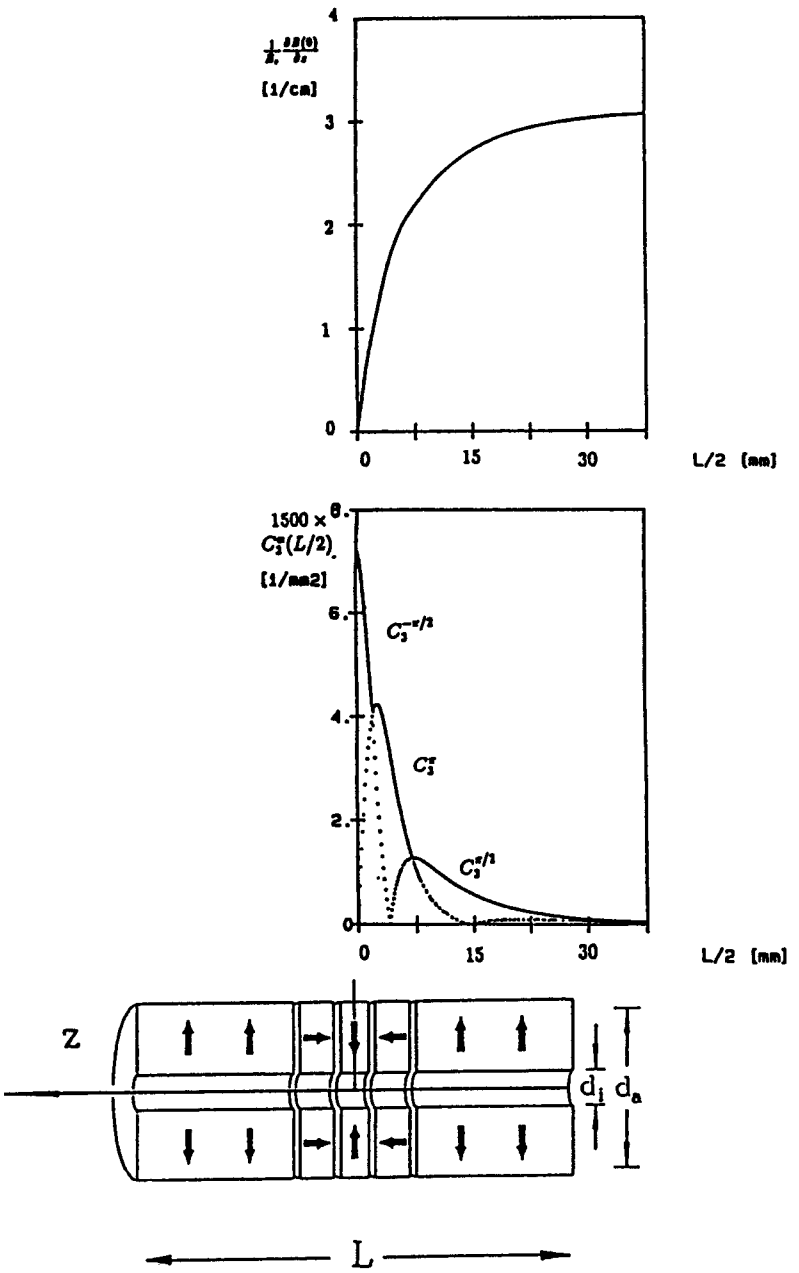

Fig. 4. Stacked cylindrical magnets ($d_i = 10$ mm, $d_a = 50$ mm) for a strong quadrupole field at the origin in the middle of the assembly. The contribution of a cylindrical element is $\Delta C_2^{\alpha} = 3C_3^{\alpha}\Delta z$. The ring with magnetisation angle α ($\alpha = \pm\pi/2$ or π) which gives maximum contribution is selected and the assembly constructed.

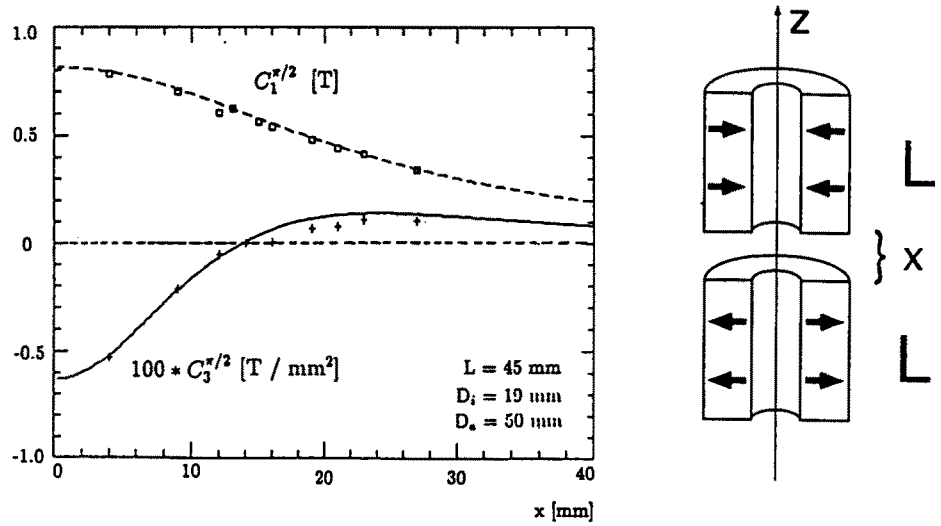

Fig. 5. C_1 (dipole) and C_3 (hexapole) coefficients for two radially magnetised rings as a function of mutual separation x ($d_i = 19$ mm, $d_a = 50$ mm, $L = 45$ mm). Note that $C_3^{\pi/2}$ vanishes for cylinders separated by $x = 14$ mm.

First we tested the assumption of linearity, which was valid even in the case of maximum opposing fields. Then we checked the lowest order C_l^{α}-coefficients and their parameter dependence. As an example we show the measurements of the magnetic dipole and hexapole contributions for two oppositely orientated radially magnetised rings ($L = 45$ mm) as a function of their mutual separation x (fig. 5). They are in good agreement with the theoretical predictions (full curves). Choosing a suitable distance can lead to higher purity of the dipole arrangement zeroing the $C_3^{\pi/2}$ contribution at the expense of about 20% field strength, as can be seen in fig. 5.

A second example is showing the measured C_2^{π}-coefficient or quadrupole field strength of two cylindrical components again as a function of their seperation (fig. 6). We observe a high degree of agreement between the predicted curve (full line) and the actual measurements (squares).

6. Discussion

Although we have discussed radially magnetised rings with continuously varying magnetisation, the perturbations caused by the technically necessary segmentation can be included in our analysis [13]. For example division of a full ring into eight uniformly magnetised segments causes a reduction by a factor 0.98 in total quadrupole field strength and introduces the first extra perturbations at the coefficient C_{2M}, M being the number of segments.

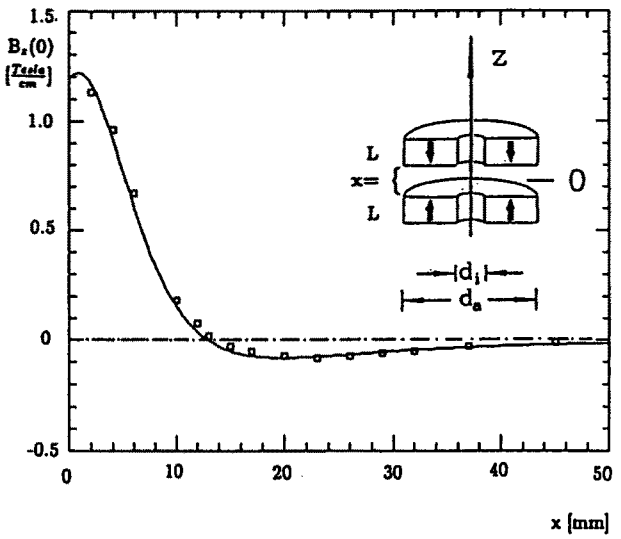

Fig. 6. The magnetic field gradient at the origin in the z direction of two axially magnetised rings as a function of their mutual separation x ($d_i = 9.4\,\text{mm}$, $d_a = 19.4\,\text{mm}$, $L = 5.0\,\text{mm}$, $B_r = 1.05\,\text{T}$).

7. Applications

Useful applications of cylindrical magnetic configurations include Penning traps and traps for neutral atoms.

A Penning ion trap for lighter particles is currently under construction in our lab. The magnetic field will be provided by permanent magnets. In a first version a field of 0.6 T with a homogeneity better than 1% in a $5 \times 5 \times 5\ \text{mm}^3$ region produced by a cylindrical stack of the aforementioned type is used. The homogeneity is well in the regime of standard shim coils for further improvement of field quality. In particular a combination with the cylindrical electrical quadrupole trap (fig. 7) as employed by Gabrielse and coworkers [14] should be beneficial.

Secondly a stacked quadrupole is considered as low field seeker trap. Due to the strong binding of the atom to the field center in the steep gradient field quantized motion can be expected for neutral atoms with negative dipole moments at temperatures in the μK domain [15]. The field zero in the middle of the trap opens a possible decay channel by which the quantum states acquire some finite width. Nevertheless we hope to be able to study laser-cooled atoms like Cs in such a trap. Techniques learned in the procedure will also have relevance to the trapping of atomic (anti)hydrogen.

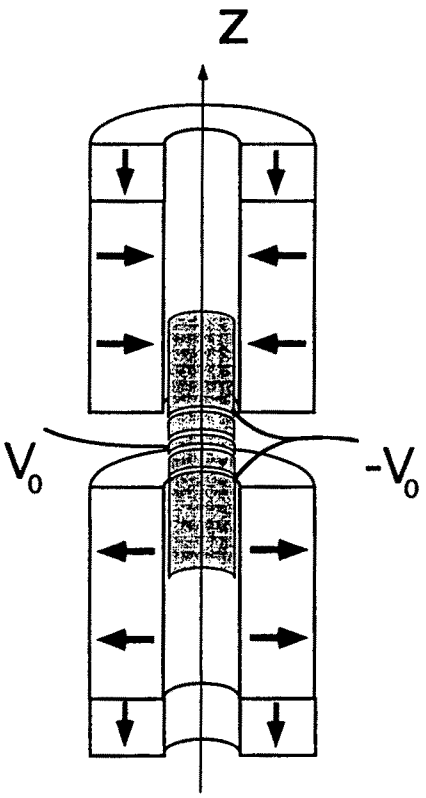

Fig. 7. Combination of cylindrical electrodes [14] and a cylindrical magnet assembly for a Penning ion trap.

8. Conclusion

The generation of strong fields by pure REM materials can be treated analytically with no need for lengthy computations. This was demonstrated with two specific examples of cylindrical rings being of interest for trapping charged and neutral species. In high precision experiments where good knowledge of the magnetic fields is required the potential of the REM has not been exploited so far. Low costs for the set-up as well as the simple maintenance of such an experiment favour the use of REM material in comparison with superconducting coils, where limited precision is tolerable.

Acknowledgement

We thank V. Gomer for his assistance with some of the measurements. This work was funded by the Deutsche Forschungsgemeinschaft.

Acknowledgement

We thank V. Gomer for his assistance with some of the measurements. This work was funded by the Deutsche Forschungsgemeinschaft.

References

[1] L.S. Brown and G. Gabrielse, Rev. Mod. Phys. 58 (1986) 233.
[2] T. Bergeman, G. Erez and H. Metcalf, Phys. Rev. A35 (1987) 1535.
[3] N. Masuhara, M.J. Doyle, J.C. Sandberg, D. Kleppner, T.J. Greytak, H.F. Hess and G.P. Kochanski, Phys. Rev. Lett. 61 (1988) 935.
[4] R. v. Roijen, J.J. Berkhout, S. Jaakhola and J.T.M. Walraven, Phys. Rev. Lett. 66 (1988) 931.
[5] K.J. Kügler, K. Moritz, W. Paul and U. Trinks, Nucl. Instr. Meth. 228 (1985) 240.
[6] D. Thompson, R.V.E. Lovelace and D.M. Lee, J. Opt. Soc. Am. B6 (1989) 2227.
[7] E.L. Raab, M. Prentiss, A. Cable, S. Chu and D.E. Pritchard, Phys. Rev. Lett. 59 (1987) 2631.
[8] K. Halbach, Nucl. Instr. Meth. 169 (1980) 1.
[9] K. Wagener-Gutheil, Doktorarbeit KFA Jülich, Jül-Spez-539, ISSN 0343-7639 (1989).
[10] K. Trines, K.H. Wroblewski and C. Falland, Internal Report, DESY Hamburg (1991).
[11] Catalogue Vacuumschmelze: *Selten-Erd- Magnetwerkstoffe*, Hanau, Germany (1989);
Catalogue Krupp Widia: *Dauermagnetische Werkstoffe und Bauteile*, Essen, Germany (1989);
Catalogue IBS Magnet: *Die Welt des Magnetismus*, Berlin, Germany (1990);
Catalogue Magnetphysik, Dr. Steingroever, Köln, Germany (1988).
[12] J.D. Jackson, *Classical Electrodynamics* (Wiley, New York, 1975).
[13] V. Frerichs, W.G. Kaenders and D. Meschede, Appl. Phys. A55 (1992) 242.
[14] G. Gabrielse, L. Haarsma and S.L. Rolston, J. Mass Spectrom. Ion Proc. 88 (1989) 319.
[15] T. Bergeman, D. McNicholl, K. Kycia, H. Metcalf and N. Balazs, J. Opt. Soc. Am. B6 (1989) 2249.